

1231736

THE UNITED STATES OF AMERICA

TO ALL TO WHOM THESE PRESENTS, SHALL COME;

UNITED STATES DEPARTMENT OF COMMERCE
United States Patent and Trademark Office

September 29, 2004

THIS IS TO CERTIFY THAT ANNEXED HERETO IS A TRUE COPY FROM THE RECORDS OF THE UNITED STATES PATENT AND TRADEMARK OFFICE OF THOSE PAPERS OF THE BELOW IDENTIFIED PATENT APPLICATION THAT MET THE REQUIREMENTS TO BE GRANTED A FILING DATE.

APPLICATION NUMBER: 60/467,177
FILING DATE: May 01, 2003
RELATED PCT APPLICATION NUMBER: PCT/US04/13852

BEST AVAILABLE COPY

Certified by

Jon W Dudas

Acting Under Secretary of Commerce
for Intellectual Property
and Acting Director of the U.S.
Patent and Trademark Office



JC901 U.S. PTO
05/01/03

050203 60467177 PTO/SE 18 (10-01)

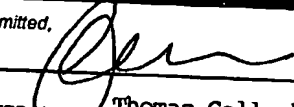
Under the Paperwork Reduction Act of 1995, no persons are required to respond to a collection of information unless it displays a valid OMB control number.
Approved for use through 10/31/2002. OMB 0651-0032
U.S. Patent and Trademark Office; U.S. DEPARTMENT OF COMMERCE

PROVISIONAL APPLICATION FOR PATENT COVER SHEET

This is a request for filing a PROVISIONAL APPLICATION FOR PATENT under 37 CFR 1.53(c).
Express Mail Label No. **EL15342255US**

JC901 U.S. PTO
05/01/03

INVENTOR(S)					
Given Name (first and middle [if any])		Family Name or Surname		Residence (City and either State or Foreign Country)	
DALE		LUDWIG		Randolph, New Jersey	
<input type="checkbox"/> Additional inventors are being named on the _____ separately numbered sheets attached hereto					
TITLE OF THE INVENTION (500 characters max) Fully Human Antibodies Directed Against the Human Insulin - like Growth Factor - 1 Receptor					
Direct all correspondence to: CORRESPONDENCE ADDRESS					
<input type="checkbox"/> Customer Number		Type Customer Number here		Place Customer Number Bar Code Label here	
<input type="checkbox"/> Firm or Individual Name		Thomas C. Gallagher			
Address		ImClone Systems Incorporated			
Address		180 Varick Street			
City		New York		State	NY
Country		USA		ZIP	10014
		Telephone	646-638-5031	Fax	212-645-1405
ENCLOSED APPLICATION PARTS (check all that apply)					
<input checked="" type="checkbox"/> Specification Number of Pages		27		<input type="checkbox"/> CD(s), Number	
<input checked="" type="checkbox"/> Drawing(s) Number of Sheets		17		<input type="checkbox"/> Other (specify)	
<input type="checkbox"/> Application Data Sheet. See 37 CFR 1.76					
METHOD OF PAYMENT OF FILING FEES FOR THIS PROVISIONAL APPLICATION FOR PATENT					
<input checked="" type="checkbox"/> Applicant claims small entity status. See 37 CFR 1.27.				FILING FEE AMOUNT (\$)	
<input type="checkbox"/> A check or money order is enclosed to cover the filing fees					
<input checked="" type="checkbox"/> The Commissioner is hereby authorized to charge filing fees or credit any overpayment to Deposit Account Number:		09-0071		\$80.00	
<input type="checkbox"/> Payment by credit card. Form PTO-2038 is attached.					
The invention was made by an agency of the United States Government or under a contract with an agency of the United States Government.					
<input checked="" type="checkbox"/> No.					
<input type="checkbox"/> Yes, the name of the U.S. Government agency and the Government contract number are: _____					

Respectfully submitted,
SIGNATURE 
TYPED or PRINTED NAME **Thomas Gallagher**
TELEPHONE **(646) 638-5031**

Date **5/1/03**
REGISTRATION NO. **37,066**
(if appropriate)
Docket Number: **LUD-2-(P)**

USE ONLY FOR FILING A PROVISIONAL APPLICATION FOR PATENT

This collection of information is required by 37 CFR 1.51. The information is used by the public to file (and by the PTO to process) a provisional application. Confidentiality is governed by 35 U.S.C. 122 and 37 CFR 1.14. This collection is estimated to take 8 hours to complete, including gathering, preparing, and submitting the complete provisional application to the PTO. Time will vary depending upon the individual case. Any comments on the amount of time you require to complete this form and/or suggestions for reducing this burden, should be sent to the Chief Information Officer, U.S. Patent and Trademark Office, U.S. Department of Commerce, Washington, D.C. 20231. DO NOT SEND FEES OR COMPLETED FORMS TO THIS ADDRESS. SEND TO: Box Provisional Application, Assistant Commissioner for Patents, Washington, D.C. 20231.

Docket No. LUD-2-(P)

IN THE UNITED STATES PATENT AND TRADEMARK OFFICE

In re Application of: Ludwig et al.

Serial No: Not yet known

Filed: Herewith

For: Fully Human Antibodies Directed Against the Human Insulin - like Growth
Factor - 1 Receptor

**EXPRESS MAIL
CERTIFICATE OF MAILING
FOR ABOVE-IDENTIFIED APPLICATION**

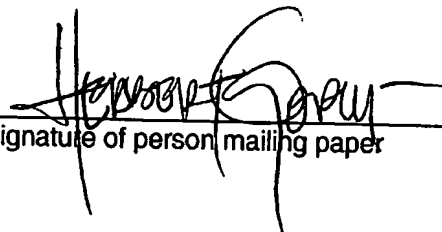
"Express Mail" mailing label number: EL153422555US

Date of Deposit: May 1, 2003

I hereby certify that the documents enclosed herewith are deposited with the United States Postal Service "Express Mail Post Office to Addressee" service under 37 C.F.R. §1.10 on the date indicated above and is addressed to the Assistant Commissioner for Patents, Washington, D.C. 20231.

Herbert Godoy

Printed Name of person mailing paper



Signature of person mailing paper

**Title: FULLY HUMAN ANTIBODIES DIRECTED AGAINST THE HUMAN
INSULIN-LIKE GROWTH FACTOR-1 RECEPTOR**

Inventor: Dale L. Ludwig, ImClone Systems Incorporated

Abstract: This invention relates to human antibodies generated against the human insulin-like growth factor-1 receptor (IGF-IR). The invention relates to derivatives of these antibodies (Fabs, single chain antibodies, bi-specific antibodies, or fusion proteins). The invention relates to nucleic acids encoding these anti-IGF-IR antibodies and their expression. The invention also relates to methods for generating anti-IGF-IR antibodies and compositions thereof for use as therapeutics or diagnostics.

BACKGROUND

The insulin-like growth factor receptor (IGF-IR) is a ubiquitous transmembrane tyrosine kinase receptor that is essential for normal fetal and post-natal growth and development. IGF-IR can stimulate cell proliferation, cell differentiation, changes in cell size, and protect cells from apoptosis. It has also been considered to be quasi-obligatory for cell transformation (reviewed in Adams et al., CMLS. 57:1050-1093, 2000; Baserga, Oncogene 19:5574-5581, 2000). The IGF-IR is located on the cell surface of most cell types and serves as the signaling molecule for growth factors IGF-I and IGF-II

(collectively termed henceforth IGFs). IGF-IR also binds insulin, albeit at three orders of magnitude lower affinity than its binding to IGFs. The IGF-IR is a pre-formed heterotetramer containing two alpha and two beta chains covalently linked by disulfide bonds. The receptor is synthesized as a single polypeptide chain of 180kd, which is then proteolytically processed into alpha (130kd) and beta (95kd) subunits. The entire alpha chain is extracellular and contains the site for ligand binding. The beta chain possesses the transmembrane domain, the tyrosine kinase domain, and a C-terminal extension that is necessary for cell differentiation and transformation, but is dispensable for mitogen signaling and protection from apoptosis.

The IGF-IR is highly similar to the insulin receptor (IR), particularly within the beta chain sequence (70% homology). Because of this homology, recent studies have demonstrated that these receptors can form hybrids containing one IR dimer and one IGF-IR dimer (Pandini et al., Clin. Canc. Res. 5:1935-1944. 1999). The formation of hybrids occurs in both normal and transformed cells and the hybrid content is dependent upon the concentration of the two homodimer receptors (IR and IGF-IR) within the cell. In one study of 39 breast cancer specimens, although both IR and IGF-IR were over-expressed in all tumor samples, hybrid receptor content consistently exceeded the levels of both homo-receptors by approximately 3-fold (Pandini et al., Clin. Canc. Res. 5:1935-1944. 1999). Although hybrid receptors are composed of IR and IGF-IR pairs, the hybrids are selective for IGFs binding, with affinity similar to IGF-IR, and only weakly bind insulin (Siddle and Soos, The IGF System. Humana Press. 199-225. 1999). These hybrids therefore can bind IGFs and transduce signals in both normal and transformed cells.

A second IGF receptor, IGF-IIR, or mannose-6-phosphate (M6P) receptor, also binds IGF-II ligand with high affinity, but lacks tyrosine kinase activity (Oates et al., Breast Cancer Res Treat. 47:269-281. 1998). Because it results in the degradation of IGF-II, it is considered a sink for IGF-II, antagonizing the growth promoting effects of this ligand. Loss of the IGF-IIR in tumor cells can enhance growth potential through release of its antagonistic effect on the binding of IGF-II with the IGF-IR (Byrd et al., J. Biol. Chem. 274:24408-24416. 1999). Endocrine expression of IGF-I is regulated primarily by growth hormone and produced in the liver, but recent evidence suggests that many tissue types are also capable of expressing IGF-I. This ligand is therefore subjected to endocrine and paracrine regulation, as well as autocrine in the case of many types of tumor cells (Yu and Rohan, J. NCI. 92:1472-1489.2000).

Six IGF binding proteins (IGFBPs) with specific binding affinities for the IGFs have been identified in serum (Yu and Rohan, J. NCI. 92:1472-1489.2000). IGFBPs can either enhance or inhibit the action of IGFs, as determined by the molecular structures of the binding proteins as a result of post-translational modifications. Their primary roles are for transport of IGFs, protection of IGFs from proteolytic degradation, and regulation of the interaction of IGFs with IGF-IR. Only about 1% of serum IGF-I is present as free ligand, the remainder is associated with IGFBPs (Yu and Rohan, J. NCI. 92:1472-1489.2000).

Upon binding of ligand (IGFs), the IGF-IR undergoes autophosphorylation at conserved tyrosine residues within the catalytic domain of the beta chain. Subsequent phosphorylation of additional tyrosine residues within the beta chain provides docking sites for the recruitment of downstream molecules critical to the signaling cascade. The

principle pathways for transduction of the IGF signal are mitogen activated protein kinase (MAPK) and phosphatidylinositol 3-kinase (PI3K) (reviewed in Blakesley et al., In: The IGF System. Humana Press. 143-163. 1999). The MAPK pathway is primarily responsible for the mitogenic signal elicited following IGFs stimulation and PI3K is responsible for the IGF-dependent induction of anti-apoptotic or survival processes.

A key role of IGF-IR signaling is its anti-apoptotic or survival function. Activated IGF-IR signals PI3K and downstream phosphorylation of Akt, or protein kinase B. Akt can effectively block, through phosphorylation, molecules such as BAD, which are essential for the initiation of programmed cell death, and inhibit initiation of apoptosis (Datta et al., Cell. 91:231-241. 1997). Apoptosis is an important cellular mechanism that is critical to normal developmental processes (Oppenheim. Annu. Rev. Neurosci. 14:453-501. 1991). It is a key mechanism for effecting the elimination of severely damaged cells and reducing the potential persistence of mutagenic lesions that may promote tumorigenesis. To this end, it has been demonstrated that activation of IGFs signaling can promote the formation of spontaneous tumors in a mouse transgenic model (DiGiovanni et al. Cancer Res. 60:1561-1570. 2000). Furthermore, IGF over-expression can rescue cells from chemotherapy induced cell death and may be an important factor in tumor cell drug resistance (Gooch et al., Breast Cancer Treat. 56:1-10. 1999). Consequently, modulation of the IGF signaling pathway has been shown to increase the sensitivity of tumor cells to chemotherapeutic agents (Benini et al., Clinical Cancer Res. 7:1790-1797. 2001).

A large number of research and clinical studies have implicated the IGF-IR and its ligands (IGFs) in the development, maintenance, and progression of cancer. In tumor

cells, over-expression of the receptor, often in concert with over-expression of IGF ligands, leads to potentiation of these signals and, as a result, enhanced cell proliferation and survival. IGF-I and IGF-II have been shown to be strong mitogens for a wide variety of cancer cell lines including prostate (Nickerson et al. Cancer Res. 61:6276-6280. 2001, Hellawell et al., Cancer Res. 62:2942-2950. 2002), breast (Gooch et al., Breast Cancer Res. Treat. 56:1-10. 1999), lung, colon (Hassan and Macaulay. Ann. Oncol. 13:349-356. 2002), stomach, leukemia, pancreas, brain, myeloma (Ge and Rudikoff. Blood. 96:2856-2861. 2000), melanoma (All-Ericsson et al., Invest. Ophthalmol. Vis. Sci. 43:1-8. 2002), and ovary (reviewed in: Macaulay. Br. J. Cancer. 65:311-320. 1990) and this effect is mediated through the IGF-IR. High circulating levels of IGF-I in serum have been associated with an increased risk of breast, prostate, and colon cancer (Pollak. Eur. J. Cancer. 36:1224-1228. 2000). In a mouse model of colon cancer, increases in circulating IGF-I levels *in vivo* led to a significant increase in the incidence of tumor growth and metastasis (Wu et al., Cancer Res. 62: 1030-1035. 2002). Constitutive expression of IGF-I in epidermal basal cells of transgenic mice has been shown to promote spontaneous tumor formation (DiGiovanni et al. Cancer Res. 60:1561-1570. 2000; Bol et al., Oncogene. 14:1725-1734. 1997). Over-expression of IGF-II in cell lines and tumors occurs with high frequency and may result from loss of genomic imprinting of the IGF-II gene (Yaginuma et al., Oncology. 54:502-507. 1997). Receptor over-expression has been demonstrated in many diverse human tumor types including lung (Quinn et al., J. Biol. Chem. 271:11477-11483. 1996), breast (Cullen et al., Cancer Res. 50: 48-53, 1990; Peyrat and Bonnetterre. Cancer Res. 22:59-67. 1992; Lee and Yee. Biomed & Pharmacother. 49:415-421. 1995), sarcoma (van Valen et al., J. Cancer Res. Clin. Oncol.

118:269-275. 1992; Scotlandi et al., *Cancer Res.* 56:4570-4574. 1996), prostate (Nickerson et al., *Cancer Res.* 61:6276-6280. 2001), and colon (Hassan and Macaulay. *Annals Oncol.* 13:349-356. 2002). In addition, highly metastatic cancer cells have been shown to possess higher expression of IGF-II and IGF-IR than tumor cells that are less prone to metastasize (Guerra et al., *Int. J. Cancer.* 65:812-820. 1996). A critical role of the IGF-IR in cell proliferation and transformation was demonstrated in experiments of IGF-IR knockout derived mouse embryo fibroblasts. These primary cells grow at significantly reduced rates in culture medium containing 10% serum and fail to transform by a variety of oncogenes including SV40 Large T (Sell et al., *Mol. Cell. Biol.* 3604-3612. 1994). Recently it was demonstrated that resistance to the drug Herceptin in some forms of breast cancer may be due to activation of IGF-IR signaling in those cancers (Lu, et al., *J. Natl. Cancer Inst.* 93:1852-1857. 2001). Over-expression or activation of IGF-IR may therefore not only be a major determinant in tumorigenicity, but also in tumor cell drug resistance.

Activation of the IGF system has also been implicated in several pathological conditions besides cancer, including acromegaly (Drange and Melmed. In: *The IGF System.* Humana Press. 699-720. 1999), retinal neovascularization (Smith et al., *Nature Med.* 12:1390-1395. 1999), and psoriasis (Wraight et al., *Nature Biotech.* 18:521-526. 2000). In the latter study, an antisense oligonucleotide preparation targeting the IGF-IR was effective in significantly inhibiting the hyperproliferation of epidermal cells in human psoriatic skin grafts in a mouse model, suggesting that anti-IGF-IR therapies may be an effective treatment for this chronic disorder.

A variety of strategies have been developed to inhibit the IGF-IR signaling pathway in cells. Antisense oligonucleotides have been effective *in vitro* and in experimental mouse models, as shown above for psoriasis. In addition, inhibitory peptides targeting the IGF-IR have been generated that possess anti-proliferative activity *in vitro* and *in vivo* (Pietrkowski et al., Cancer Res. 52:6447-6451. 1992; Hickling et al., J. Am. Soc. Nephrol. 11:2027-35. 2000). A synthetic peptide sequence from the C-terminus of IGF-IR has been shown to induce apoptosis and significantly inhibit tumor growth (Reiss et al., J. Cell. Phys. 181:124-135. 1999). Several dominant-negative mutants of the IGF-IR have also been generated which, upon over-expression in tumor cell lines, compete with wild-type IGF-IR for ligand and effectively inhibit tumor cell growth *in vitro* and *in vivo* (Scotlandi et al., Int. J. Cancer. 101:11-6. 2002; Seely et al., BMC. Cancer. 2:15. 2002). Additionally, a soluble form of the IGF-IR has also been demonstrated to inhibit tumor growth *in vivo* (D'Ambrosio et al., Cancer Res. 56:4013-4020. 1996). Antibodies directed against the human IGF-IR have also been shown to inhibit tumor cell proliferation *in vitro* and tumorigenesis *in vivo* including cell lines derived from breast cancer (Arteaga and Osborne, cancer Res. 49:6237-6241. 1989), Ewing's osteosarcoma (Scotlandi et al., Cancer Res. 58:4127-4131. 1998), and melanoma (Furlanetto et al., Cancer Res. 53:2522-2526. 1993). Antibodies are attractive therapeutics chiefly because of they 1) can possess high selectivity for a particular protein antigen, 2) are capable of exhibiting high affinity binding to the antigen, 3) possess long half-lives *in vivo*, and, since they are natural immune products, should 4) exhibit low *in vivo* toxicity (Park and Smolen. In: Advances in Protein Chemistry. Academic Press. pp:360-421. 2001). Antibodies derived from non-human sources, eg: mouse, may,

however, effect a directed immune response against the therapeutic antibody, following repeated application, thereby neutralizing the antibody's effectiveness. Fully human antibodies offer the greatest potential for success as human therapeutics since they would likely be less immunogenic than murine or chimeric antibodies in humans, similar to naturally occurring immuno-responsive antibodies. To this end, there is a need to develop high affinity human anti-IGF-IR monoclonal antibodies for therapeutic use.

METHODS AND RESULTS

Selection and engineering of anti-human IGF-IR monoclonal antibodies.

In order to isolate high affinity antibodies to the human IGF-I receptor, recombinant extracellular portion of human IGF-IR was used to screen a human naïve (non-immunized) bacteriophage Fab library containing 3.7×10^{10} unique clones (de Haard, et al., J. Biol. Chem. 274:18218-18230. 1999). Soluble IGF-IR (50ug/ml) was coated onto tubes and blocked with 3% milk/PBS at 37 degrees for 1 hour. Phage were prepared by growing library stock to log phase culture, rescuing with M13K07 helper phage, and amplifying overnight at 30°C in 2YTAK culture medium at containing ampicillin and kanamycin selection. The resulting phage preparation was precipitated in 4% PEG/0.5M NaCl and resuspended in 3% milk/PBS. The immobilized receptors were then incubated with phage preparation for 1 hour at room temperature. Afterwards, the tubes were washed 10 times with PBST (PBS containing 0.1% Tween-20) followed by 10 times with PBS. The bound phage was eluted at RT for 10 min with 1 ml of a freshly prepared solution of 100 mM triethylamine. The eluted phage were incubated with 10 ml of mid-log phase TG1 cells at 37°C for 30 min stationary and 30 min shaking. The infected TG1

cells were pelleted and plated onto several large 2YTAG plates and incubated overnight at 30°C. All colonies that grew on the plates were scraped into 3 to 5 ml of 2YTA medium, mixed with glycerol (final concentration: 10%), aliquoted and stored at -70°C. For second round selection, 100 µl of the phage stock was added to 25 ml of 2YTAG medium and grown to mid-log phase. The culture was rescued with M13K07 helper phage, amplified, precipitated, and used for selection following the procedure described above, but with reduced concentration (5 µg/ml) of IGF-IR immobilized onto tubes and increasing the numbers of washes following the binding process. A total of two rounds of selection were performed.

Individual TG1 clones were picked and grown at 37°C in 96 well plates and rescued with M13K07 helper phage as described above. The amplified phage preparation was blocked with 1/6 volume of 18% milk/PBS at RT for 1 h and added to Maxi-sorb 96-well microtiter plates (Nunc) coated with IGF-IR (1 µg/ml x 100 µl). After incubation at RT for 1 h the plates were washed 3 times with PBST and incubated with a mouse anti-M13 phage-HRP conjugate (Amersham Pharmacia Biotech, Piscataway, NJ). The plates were washed 5 times, TMB peroxidase substrate (KPL, Gaithersburg, MD) added, and the absorbance at 450 nm read using a microplate reader (Molecular Device, Sunnyvale, CA). From 2 rounds of selection, 80% of independent clones were positive for binding to IGF-IR.

The diversity of the anti-IGF-IR Fab clones after the second round of selection was analyzed by restriction enzyme digestion pattern (*i.e.*, DNA fingerprint). The Fab gene insert of individual clones was PCR amplified using primers: PUC19 reverse, 5' AGCGGATAACAATTTACACAGG 3'; and fdtet seq, 5' GTCGTCTTTCCAGACGT-

TAGT 3' which are specific for sequences flanking the unique Fab gene regions within the phage vector. Each amplified product was digested with a frequent-cutting enzyme, *Bst*NI, and analyzed on a 3% agarose gel. A total of 25 distinct patterns were identified. DNA sequences of representative clones from each digestion pattern were determined by dideoxynucleotide sequencing.

Plasmids from individual clones exhibiting positive binding to IGF-IR and unique DNA profile were used to transform a nonsuppressor *E.coli* host HB2151. Expression of the Fab fragments in HB2151 was induced by culturing the cells in 2YTA medium containing 1 mM isopropyl-1-thio- β -D-galactopyranoside (IPTG, Sigma) at 30°C. A periplasmic extract of the cells was prepared by resuspending the cell pellet in 25 mM Tris (pH 7.5) containing 20% (w/v) sucrose, 200 mM NaCl, 1 mM EDTA and 0.1 mM PMSF, followed by incubation at 4°C with gentle shaking for 1 h. After centrifugation at 15,000 rpm for 15 min, the soluble Fab protein was purified from the supernatant by affinity chromatography using Protein G column followed the manufacturer's protocol (Amersham Pharmacia Biotech).

Candidate binding Fab clones were screened for competitive blocking of radiolabeled human IGF-I ligand to immobilized IGF-IR (100ng/well) coated onto 96 strip-well plates. Fab preparations were diluted and incubated with IGF-IR plates for 0.5-1 hour at room temperature in PBS/0.1%BSA. Forty 40pM of 125 I-IGF-I was then added and the plates incubated an additional 90 minutes. Wells were then washed 3 times with ice-cold PBS/0.1% BSA, dried, and then counted in a gamma scintillation counter. Candidates that exhibited greater than 30% inhibition of control radiolabeled ligand binding in single point assay were selected and *in vitro* blocking titers determined. Four

clones were identified. Of these, only Fab clone 2F8 was shown to inhibit ligand binding by more than 50%, with an IC_{50} of approximately 200nM, and it was selected for conversion to full length IgG1 format. The heavy chain variable region sequence and translated amino acid sequence for 2F8 is shown in Figures 1 and 2, respectively. The DNA sequence and translated polypeptide sequence of the 2F8 heavy chain engineered as full length IgG1 are shown in Figures 3 and 4, respectively.

Fab 2F8 sequencing determined that this Fab possessed a lambda light chain constant region. The DNA sequence and translated amino acid sequence of the 2F8 light chain are shown in Figures 5 and 6, respectively. The sequences for full-length lambda light chain format are shown in Figures 7 and 8. Binding kinetic analysis was performed on 2F8 IgG using a BIAcore unit. This antibody was determined to bind to the IGF-IR with an affinity of 0.5 –1 nM ($0.5-1 \times 10^{-9}$ M).

In order to improve the affinity of this antibody, a second generation Fab phage library was generated in which the 2F8 heavy chain was conserved and the light chain was varied to a diversity of greater than 10^8 unique species. This method is termed light chain shuffling and has been used successfully to affinity mature selected antibodies for a given target antigen (Chames, et al., J. Immunol. 169:1110-1118. 2002). This library was then screened for binding to the human IGF-IR (10ug/ml) following procedures as described above, and the panning process repeated an additional three rounds with reduced IGF-IR concentration (2ug/ml) for enrichment of high affinity binding Fabs. Seven clones were analyzed following round 4. All 7 contained the same DNA sequence and restriction digest profile. The single isolated Fab was designated A12 and shown to possess a lambda light chain constant region. The light chain DNA sequence is shown in

Figure 9 and amino acid sequence in Figure 10. Complete lambda light chain sequence and translated polypeptide sequence are shown in Figures 11 and 12, respectively. Amino acid sequence comparison of 2F8 and A12 light chains determined that the two variable regions differed by a total of 11 amino acids (refer to Figures 13 and 14). Nine of the changes were present within CDR regions, with the majority (6 amino acid residues) occurring within CDR3. A comparison of the two antibody (full IgG) affinities for the IGF-IR and their ligand blocking activity is shown in Table I.

Antibody	Binding (ED ₅₀)	Blocking (IC ₅₀)	Affinity
2F8	2.0nM	3-6nM	$K_D=6.5 \times 10^{-10}$ $K_{on}=2.8 \times 10^5$ $K_{off}=1.8 \times 10^{-4}$
A12	0.3nM	0.6-1nM	$K_D=4.1 \times 10^{-11}$ $K_{on}=7.2 \times 10^5$ $K_{off}=3.0 \times 10^{-5}$

Table 1. Antibody binding characteristics to the human IGF-IR. Binding results were determined by human IGF-IR ELISA and represent the concentration of titrated antibody necessary to achieve 50% binding relative to saturation. Blocking results represent the level of antibody necessary to inhibit 50% binding of ¹²⁵I-IGF-I ligand to immobilized human IGF-IR. Affinity was determined by BIAcore analysis according to manufacturer's specifications (Pharmacia BIACORE 3000). Soluble IGF-IR was immobilized on the sensorchips and antibody binding kinetics determined.

The antibody changes incurred in 2F8 light chain to generate antibody A12 effected a significantly higher affinity of A12 for IGF-IR than 2F8. Concomitantly, this increase effected a greater binding ability of A12 for the receptor, as determined by ELISA, and at least a three-fold increase in blocking activity of ligand for immobilized receptor. Figure

15 shows a representative titration of the two anti-IGF-IR antibodies in receptor blocking assay. The activity of A12 remained the same, irrespective of whether the light chain was engineered with a human lambda or kappa class constant region. Antibody A12 engineered with a lambda class light chain was utilized in all subsequent procedures. In this assay, A12 inhibited the binding of radiolabeled IGF-I to the IGF-IR to a greater extent than competition with cold ligand. The activity of 2F8 was comparable to competition with cold ligand. This is consistent with the relative affinities of the two antibodies (see Table 1) and IGF-I (0.5-1nM).

Engineering and expression of fully human IgG1 anti-IGF-IR antibodies from Fab clones.

The DNA sequences encoding the heavy and light chain genes of Fabs 2F8 and A12 were amplified by polymerase chain reaction (PCR) using the Boehringer Mannheim Expand kit according to manufacturer's instructions. Forward and reverse primers contained sequences for restriction endonuclease sites for cloning into mammalian expression vectors. The recipient vector for the heavy chain contained the entire human gamma 1 constant region cDNA sequence, flanked by a strong eukaryotic promoter and a 3' polyadenylation sequence. The full-length lambda light chain sequences for 2F8 or A12 were each cloned in to a second vector possessing only the eukaryotic regulatory elements for expression in mammalian cells. A selectable marker was also present on this vector for selection of stable DNA integrants following transfection of the plasmid into mammalian cells. Forward primers were also engineered with sequences encoding a strong mammalian signal peptide sequence for proper secretion of the expressed

antibody. Following identification of properly cloned immunoglobulin gene sequences, the DNAs were sequenced and tested for expression in transient transfection. Transient transfection was performed into the COS7 primate cell line using Lipofection, according to manufacturer's specifications. At 24 or 48 post-transfection, the expression of full IgG antibody was detected in conditioned culture supernatant by anti-human-Fc binding ELISA. ELISA Plates (96 well) were prepared by coating with 100ng/well of a goat-anti-human Fc-specific polyclonal antibody (Sigma) and blocked with 5% milk/PBS overnight at 4°C. The plates were then washed 5 times with PBS. Conditioned supernatant was added to wells and incubated for 1.5 hours at room temperature. Bound antibody was detected with a goat anti-human lambda light chain-HRP antibody (Sigma) and visualized with TMB reagents and microplate reader as described above. Large scale preparation of anti-IGF-IR antibodies was achieved by either large scale transient transfection into COS cells, by scale-up of the Lipofection method or by stable transfection into a suitable host cell such as a mouse myeloma cell line (NS0, Sp2/0) or a Chinese hamster ovary cell line (CHO). Plasmid encoding the anti-IGF-IR antibodies were transfected into host cells by electroporation and selected in appropriate drug selection medium for approximately two weeks. Stably selected colonies were screened for antibody expression by anti-Fc ELISA and positive clones expanded into serum free cell culture medium. Antibody production from stably transfected cells was performed in suspension culture in spinner flasks or bioreactors for a period of up to two weeks. Antibody generated by either transient or stable transfection was purified by ProA affinity chromatography (Harlow and Lane. Antibodies. A Laboratory Manual. Cold Spring Harbor Press. 1988), eluted into a neutral buffered saline solution, and quantitated.

Determination of ligand blocking activity of anti-IGF-IR monoclonal antibodies on human tumor cells.

The anti-IGF-IR antibodies were then tested for blocking of radiolabeled ligand to native IGF-IR on human tumor cells. Assay conditions were performed according to Arteaga and Osborne (Cancer Res. 49:6237-6241.1989), with minor modifications. MCF7 human breast cancer cells were seeded into 24 well dishes, and cultured overnight. Sub-confluent monolayers were washed 2-3 times in binding buffer (Iscove's Medium/0.1% BSA) and antibody added in binding buffer. After a short incubation with the antibody at room temperature, 40pM 125I-IGF-I (approximately 40,000cpm/well) was added to each well and incubated for an additional hour with gentle agitation. The wells were then washed three times with ice-cold PBS/0.1%BSA. Monolayers were then lysed with 200ul 0.5N NaOH and counted in a gamma counter. The results are shown graphically in Figure 16. On human tumor cells, antibody A12 inhibited ligand binding to IGF-IR with an IC_{50} of 3nM (0.45ug/ml). This was slightly lower than the inhibitory activity of cold IGF-I ligand (IC_{50} = 1nM), but better than the inhibitory activity of cold IGF-II (IC_{50} = 9nM). The differences observed for the two IGF ligands can likely be attributed to the slower binding kinetics of IGF-II for the IGF-IR than ligand IGF-I (Jansson et al., J. Biol. Chem. 272:8189-8197. 1997). The IC_{50} for antibody 2F8 was determined to be 30nM (4.5ug/ml). We subsequently determined the IGF-I ligand blocking activity of the A12 antibody on several different human tumor types. The results are shown in Table 2. Antibody A12 was effective in binding to endogenous cellular

IGF-IR and inhibiting ligand binding to a range of human tumor types including cell lines from breast, pancreatic, and colorectal tissue.

The IGF-IR shares considerable homology with the insulin receptor (IR). To determine if the anti-IGF-IR antibodies were specific to this IGF-IR and did not block insulin binding, a cell-based blocking assay was performed on human ZR-75I breast cancer cells. Because insulin can bind to IGF-IR, albeit at three orders of magnitude lower affinity than for the IR, we utilized the human breast cancer line ZR-75I that possesses a higher IR to IGF-IR ratio in comparison to MCF7 cells. By using this line, we reasoned that insulin binding to the cells would be more indicative of specific IR binding. The assay was performed as described above for MCF7 cells and the results shown in Figure 17. Although cold insulin was able to titrate the binding of radiolabeled insulin to cells, neither 2F8 nor the high affinity A12 antibody blocked insulin binding, even at a concentration of 200nM antibody, consistent with selective binding of these antibodies to IGF-IR and not IR.

Antibody-mediated inhibition of ligand-dependent cell mitogenesis.

In order to determine if blocking of IGF-I binding to IGF-IR inhibited cellular proliferation, a mitogenic assay was performed on MCF7 breast cancer cells. The assay was performed according to Prager, et al., (Proc. Natl. Acad. Sci. U.S.A. 91:2181-2185, 1994), with some modification. MCF7 cells were plated into 96-well tissue culture plates at 5000-10000 cells/well and allowed to adhere overnight. The medium was then replaced with serum free defined medium and incubated overnight at 37°C. Cells were then incubated with IGF-I with or without antibody A12 and incubated overnight at

37°C. [^3H]Thymidine (0.25uCi) was then added to each well and incubated for 5 hours at 37°C. The supernatant was then aspirated and the cells suspended by trypsinization for 5 minutes. The cells were then collected onto a filter and washed three times with water, using a cell harvester. After drying, the filter was processed for reading in a scintillation counter. The results are shown in Figure 18. The ligand was titrated on MCF7 cells to determine the amount necessary to achieve the maximum mitogenic response.

Cell line	Cell type	Blocking IC ₅₀
MCF7	breast	3nM
T47D	breast	6nM
OV90	ovarian	6nM
BXPC3	pancreatic	20nM
HPAC	pancreatic	10nM
HT-29	colorectal	10nM
SK-ES1	Ewing sarcoma	2nM
8226	myeloma	20nM

Table 2. Inhibitory activity of antibody A12 on IGF-I ligand binding to different human tumor types

For testing the activity of antibody A12, IGF-I was added at a concentration of 5nM and the antibody titrated from 200nM to 0.05nM. Antibody A12 inhibited MCF7 mitogenesis in response to IGF-I ligand in a dose-dependent fashion, with an IC₅₀ of 6nM. Antibody A12 was then tested for mitogenic inhibition on several additional human tumor cells

lines and the results shown in Table 3. Antibody A12 was effective at inhibiting IGF-I ligand-mediated mitogenesis of a variety of human tumor cell lines, including breast cancer, colorectal cancer, and multiple myeloma.

Cell line	Cell type	IC ₅₀
MCF7	breast	6nM
T47D	breast	7nM
BT474	breast	5nM
BXPC3	pancreatic	2nM
8226	myeloma	5nM
HT-29	colorectal	6nM
SK-ES1	Ewing sarcoma	10nM

Table 3. Inhibitory activity of antibody A12 on mitogenesis of different human tumor cell lines.

Antibody-mediated inhibition of IGF-I directed receptor phosphorylation and downstream signaling.

To visualize the inhibitory effect of the anti-IGF-IR antibodies on IGF-I signaling, receptor auto-phosphorylation and downstream effector molecule phosphorylation analysis was performed in the presence or absence of antibody A12 or 2F8. The MCF7 human breast cancer cell line was selected for use due to its high IGF-IR density. Cells were plated into 10cm or 6 well culture dishes and grown to 70-80% confluence. The

monolayers were then washed twice in PBS and cultured overnight in serum free defined medium. Anti-IGF-IR antibody was then added in fresh serum-free media (100nM-10nM) and incubated cells 30 minutes before addition of ligand (10nM). Cells were incubated with ligand for 10 minutes, then placed on ice and washed with ice-cold PBS. The cells were lysed by the addition of lysis solution (50mM Tris-HCl, pH 7.4, 150mM NaCl, 1% TritonX-100, 1mM EDTA, 1mM PMSF, 0.5mM Na₃VO₄, 1µg/ml leupeptin, 1µg/ml pepstatin, and 1µg/ml aprotinin) and the cells scraped into a centrifuge tube kept on ice for 15 minutes. The lysate was then clarified by centrifugation at 4°C. Solubilized IGF-IR was then immunoprecipitated (IP) from the lysate. Antibody 3B7 (Santa Cruz) or A12 at 1ug/ml were incubated with 400ul of lysate overnight at 4°C. Immune complexes were then precipitated by the addition of ProA-sepharose beads for 2 hours at 4°C, pelleted, and washed 3 times with lysis buffer. IPs bound to the ProA beads were stripped into denaturing gel running buffer. Lysate or IP were processed for denaturing gel electrophoresis and run on a 4-12% acrylamide gel and blotted to nylon or nitrocellulose membrane by western blot according to Towbin et al., (Biotechnology. 24:145-9.1992). Tyrosine phosphorylated protein was detected on the blot using an anti-p-tyrosine antibody (Cell Signaling #9411) and an anti-mouse-HRP 2° antibody. IGF-IR was detected with monoclonal antibody C-20 (Santa Cruz). For Akt phosphorylation, phospho-Akt was detected with antibody #559029 and total Akt with #559028 (BD Pharmingen). For MAPK phosphorylation, phospho-p44/42 was detected with #9101 and total p44/42 with #9102 (Cell Signaling Tech.). Bands were visualized with the ECL reagent on X-ray film. As shown in Figure 19, auto-phosphorylation of the IGF-IR was arrested following serum deprivation and the addition of either 2F8 or A12 alone did not

induce receptor phosphorylation, thereby demonstrating a lack of detectable agonist activity. Upon the addition of 10nM IGF-I, IGF-IR phosphorylation was strongly induced. Antibody 2F8 effected an approximately 50% reduction in IGF-IR phosphorylation, whereas the high affinity antibody A12 nearly completely blocked phosphorylation. Downstream effector signaling in response to IGF-I was also inhibited by the anti-IGF-IR antibodies (Figure 20). MAPK phosphorylation was considerably inhibited by both 2F8 and A12. Phosphorylation of the anti-apoptotic molecule Akt was less sensitive to anti-IGF-IR antibody blockade with 2F8. It effected only a slight reduction in Akt phosphorylation. To the contrary, A12 significantly inhibited Akt phosphorylation, even at a concentration of 10nM. Antibody A12 was equally proficient in immunoprecipitating solubilized IGF-IR as the commercial antibody 3B7, but was A12 not capable of detecting denatured IGF-IR immobilized on nylon membranes following western blot transfer.

FACs binding analysis of monoclonal antibody A12 to tumor cell lines.

Since A12 was capable of immunoprecipitating endogenous IGF-IR, we were therefore interested in determining if A12 could also be used as detection antibody for fluorescence activated cell sorting (FACs). Human tumor cell lines were grown in culture, scraped into ice-cold PBS, and counted. Primary antibody, A12 (0.5ug), was added to approximately 5 million cells in 250ul PBS/5%FBS and incubated on ice for 1 hour. The cells were then diluted to 3mls in PBS/5%FBS, pelleted, and the supernatant aspirated. Secondary phycoerythrin (PE) -labeled goat anti-human IgG F(ab)₂ fragment was then added in 250ul PBS/5%FBS at 1:200 and incubated on ice for 60 minutes.

Afterwards, the cells were again diluted and pelleted, as before, then resuspended in 500ul PBS/5%FBS. FACs analysis was then performed on a Epics XL unit (Coulter). As shown in Figure 21, antibody A12 fully shifted the human breast cancer cell line MCF7 and the human leukemia cell line HEL. IGF-IR negative mouse embryo fibroblasts (R-cells) (obtained from R. Baserga, Thomas Jefferson University, Philadelphia, PA) served as the negative control. A12 failed to bind to these cells, indicative of antibody binding specificity for the IGF-IR. A12 did, however, bind and partially shift the mouse tumor cell line Lewis Lung carcinoma, suggesting that this anti-human IGF-IR antibody possesses some cross-reactivity for the mouse IGF-IR.

IGF-I receptor internalization following binding of antibody A12.

Antibody A12 has been shown to bind native IGF-IR on human tumor cells with high affinity. We were interested in determining if upon binding, the antibody mediated internalization and consequentially, degradation, of the bound receptor. Antibody A12 was radio-iodinated with 125 I using IODO-beads (Pierce) according to manufacturer's instructions. MCF7 human breast cancer cells were plated into 6-well plates and cultured overnight to 50% confluence. One microgram of 125 I-A12 was added to each well and incubated at 37°C or kept on ice at 4°C. Plates were incubated for 30 minutes, 90minutes, or 180minutes and each time point performed in triplicate. The culture at 4°C was held for 180minutes. At each time point, wells were washed 1x w/PBS, then stripped for 5 minutes with 100mM Glycine-HCl, 2M urea, pH 2.5. The stripped material, representing membrane bound antibody was kept on ice for counting. Wells were then washed 3 times with PBS and cells solubilized with 1N

NaOH/1%TritonX100. The solubilized fraction represented the internalized antibody. Stripped and solubilized fractions were then read on a gamma counter and plotted with standard deviation. As shown in Figure 22, the level of radioactivity internalized radioactivity increased with time in the cells cultured at 37°C, while little uptake was observed in cells maintained at 4°C where membrane transport should be severely retarded. This demonstrated that, upon binding to the IGF-IR, antibody A12 is rapidly internalized, potentially leading to a depletion of surface bound receptor. This may represent an additional means by which antibody A12 effects an inhibition of the IGF signaling mechanism, by eliciting a reduction in the level of membrane bound receptor.

Growth inhibition of human colorectal tumors alone or in combination with irenotecan (CPT-11).

We were interested to determine if the anti-IGF-IR antibodies were capable of inhibiting human tumor growth *in vivo* in a nude mouse xenograft model. Tumors were induced in 3-4 week old athymic nude (*nu/nu*) mice by subcutaneous injection of 2-3 million viable HT-29 human colorectal cancer cells in cell culture medium. The tumors were allowed to establish and antibody treatment started when the tumor volume reached 200mm³. Ten animals were injected with tumor cells per treatment group. Antibody was injected intraperitoneally (IP) every three days at 1mg or 0.5mg in 0.5ml TBS. The drug irenotecan (CPT-11) (LKT Laboratories) was injected IP (100mg/kg) once a week for four weeks from the initiation of antibody treatment. Control animals received a class matched irrelevant human IgG antibody. Tumor measurements were performed at regular intervals using Vernier calipers, measuring height, width, and length and calculated to

determine the total tumor volume. The study was terminated when control tumors reached 3000mm^3 . As shown in Figure 23, doses of antibody 2F8 at either 0.5mg or 1mg every three days effected a significant inhibition ($P < 0.05$) of tumor growth in this model. There was no statistical difference between the tumor sizes from groups treated with 0.5 or 1mg A12 and the response were similar to treatment with CPT-11 alone. When A12 and CPT-11 were given together the combination resulted in greater inhibition of tumor growth (72% decrease), demonstrating that anti-IGF-IR therapy could enhance the anti-tumor activity of the chemotherapeutic agent CPT-11 on tumor growth.

Anti-tumor activity of antibody A12 on human colorectal tumors in vivo.

Antibody A12 possesses a 10-fold higher affinity for the IGF-IR than antibody 2F8. Since significant tumor inhibition was observed *in vivo* with antibody 2F8, we investigated the activity of A12 on the growth of the human colorectal cancer line HT-29 in a mouse xenograft model. Tumors were induced as previously described, and antibody treatment initiated once tumors were established (200mm^3 size). Antibody treatment was then given at a concentration of 1 mg, 100ug, or 10ug every three days throughout the duration of the experiment. Ten animals were used per treatment group and control animals received a class match IgG control antibody. As shown in Figure 24, antibody A12 effected a 74% reduction in tumor growth compared to control ($P < 0.05$). This demonstrated that A12 was effective as a single therapeutic at inhibiting colorectal tumor growth in this xenograft model. A clear dose-response effect was noted in this experiment. Anti-tumor activity was also observed with a dose of 100ug A12.

Activity of antibody A12 on human breast cancer *in vivo* in a xenograft tumor model.

Antibody A12 exhibited strong inhibitory activity on the IGF-dependent mitogenic stimulation and proliferation of MCF7 cells *in vitro*. In order to assess its activity on MCF7 tumor growth *in vivo*, a mouse xenograft tumor model was utilized. MCF7 cells were originally isolated from an estrogen-dependent human tumor and require exogenously added estrogen for maintenance and growth *in vivo*. Nude mice were implanted with biodegradable estrogen pellets (0.72mg 17- β -estradiol/pellet, 60 day release). In addition, at the time of subcutaneous tumor cell injection, the mice were also injected in the right flank subcutaneously with 0.5mg of estradiol in a 50ul suspension of sesame seed oil. Tumors were allowed to establish a size of approximately 150mm³ before antibody treatment was initiated. Antibody was injected at 1 mg, 100ug, and 10ug doses every three days and continued for the duration of the experiment. At 29 days, treatment of animals with 1 mg of A12 effected an 89% reduction in tumor growth. Minimal growth was apparent for the established tumors in this treatment group. A dose dependent response was noted for A12 treatments in this model. The study demonstrated that A12 was effective in significantly reducing the growth of a human breast cancer cell line *in vivo*.

DISCUSSION

The IGF-I receptor signaling pathway has been extensively demonstrated to be a causative factor in the development of cancer and several other diseases. Targeted inhibition of this pathway using monoclonal antibodies has been shown effective *in vitro* and *in vivo* on a variety of human tumor cell lines. However, antibodies developed using

non-human hosts such as mice not ideal for chronic therapeutic use due to the high likelihood of a directed immune response being elicited against the therapeutic antibody, so called human anti-mouse antibody response (HAMA). Even chimeric antibodies in which a murine variable region is molecularly linked to a human immunoglobulin class constant region may also elicit an anti-chimeric immune response (HACA). In this regard only fully human antibodies exhibit the greatest potential for long term therapeutic application since they would not be anticipated to elicit a direct immune response any greater than an antibody generated naturally through acquired immunity.

We have successfully generated first and second generation fully human monoclonal antibodies, 2F8 and A12, respectively, which bind specifically to the human IGF-I receptor and block ligand (IGF-I and IGF-II) binding. Both antibodies have been shown to thus inhibit ligand-mediated receptor phosphorylation and downstream cellular signaling through the MAPK and Akt pathways. Because of its higher affinity, antibody A12 is significantly more effective at inhibiting IGF-I signaling as determined by *in vitro* assay. The two antibodies differ only by a total of 11 amino acid residues within the light chain variable region. The bulk of these changes occurred within CDR3 of the light chain. Selection of A12 was performed by re-selection of the 2F8 light chain by a method called light chain shuffling. The change in light chain from 2F8 to A12, effected a greater than 10-fold increase in affinity of the antibody for the IGF-IR (refer to Table 1).

Antibody A12 was demonstrated to block ligand binding and signaling in a variety of human tumor cell lines including pancreatic, breast, colorectal, and sarcoma. This is consistent with literature reports that divers human tumor types have been shown

to rely upon IGF-IR signaling for enhanced tumor cell proliferation and protection from apoptosis.

By antibody internalization assay, we determined that following binding to IGF-IR on the surface of human tumor cells, antibody A12 is rapidly internalized into the cell. In doing so, it is anticipated that the levels of surface bound IGF-IR are rapidly diminished. This may be one mechanism by which A12 exerts a negative effect on IGF signaling in tumor cell lines, by effectively titrating the level of receptor on the tumor cell surface.

The anti-IGF-IR antibodies may also be useful as diagnostic tools. In this regard, we demonstrated that A12 could successfully immunoprecipitate IGF-IR from cellular lysates. Furthermore, we demonstrated that antibody A12 selectively bound to cells that express the IGF-IR as visualized by FACs analysis. This study determined that A12 could weakly recognize the mouse form of the IGF-IR within the Lewis lung carcinoma. We have also recently determined that A12 can selectively stain IGF-IR on paraffin and frozen fixed tissue sections by immunohistochemical methods (data not shown).

Base on the *in vitro* results demonstrating the effectiveness of the anti-IGF-IR antibodies on different human tumor types, we were interested in the potential of these antibodies for inhibiting tumor growth *in vivo*. Using the nude mouse xenograft model, we tested the antibody 2F8 alone and in combination with a chemotherapeutic agent (CPT-11) on a human colorectal cancer cell line. This antibody significantly inhibited tumor growth with doses of 0.5mg to 1mg/ injection. Combination of antibody 2F8 with CPT-11 effected a 72% reduction in tumor volume, demonstrating that 2F8 can enhance the effectiveness of this chemotherapeutic agent. The high affinity antibody A12 was

subsequently tested alone in a dose response assessment in the colorectal cancer xenograft model. Antibody A12 alone effected at 74% reduction in tumor growth and the activity was dose-dependent. We then tested A12 alone on a human breast cancer xenograft model. Antibody A12, in this model, effected an 89% reduction in tumor volume. These results demonstrate the effectiveness of this high affinity antibody on modulating tumor growth *in vivo* by blocking the IGF-IR signaling pathway. A12 was effective on colorectal and breast cancer growth, both *in vitro* and *in vivo*.

Mechanistically, the fully human antibodies 2F8 and A12 display high affinity for the human IGF-IR and competes with its ligands, IGF-I and IGF-II for binding. In turn, these antibodies inhibit ligand-mediated signal transduction of cell proliferation and survival pathways. Antibody A12, upon binding to the IGF-IR was shown to rapidly internalize, presumably by stimulating receptor internalization, and mediated subsequent receptor degradation. As a result, antibody A12 may therefore effect a reduction in the level of IGF-IR on the tumor cell surface, and thus reduce the number of receptor molecules available for ligand binding. By directly inhibiting tumor cell proliferation and survival, these antibodies significantly inhibited the growth of colorectal and breast tumors *in vivo*. Anti-IGF-IR antibody treatment alone, or in combination with a chemotherapeutic agent, exhibits potent anti-tumor activity. Because they are engineered as fully human monoclonal antibodies, they are likely to exhibit low immunoreactivity in humans *in vivo*, and therefore represent good candidate molecules for therapeutic intervention in human diseases in which activation of the IGF-IR plays a critical role.

GAGGTCCAGCTGGTGCAGTCTGGGGCTGAGGTGAAGAAGCCTGGGTCCTC	50
GGTGAAGGTCTCCTGCAAGGCTTCTGGAGGCACCTTCAGCAGCTATGCTA	100
TCAGCTGGGTGCGACAGGCCCCTGGACAAGGGCTTGAGTGGATGGGAGGG	150
ATCATCCCTATCTTTGGTACAGCAAATACGCACAGAAGTTCCAGGGCAG	200
AGTCACGATTACCGCGGACAAATCCACGAGCACAGCCTACATGGAGCTGA	250
GCAGCCTGAGATCTGAGGACACGGCCGTGTATTACTGTGCGAGAGCGCCA	300
TTACGATTTTGGAGTGGTCCACCCAAGACCACTACTACTACTACTACAT	350
GGACGTCTGGGGCAAAGGGACCACGGTCACCGTCTCAAGC	390

Figure 1. 2F8 Heavy chain variable region DNA sequence

EVQLVQSGAEVKKPGSSSVKVSCKASGGTFSS <u>SYAI</u> SWVRQAPGQGLEWM <u>GG</u>	50
<u>IIP</u> IFGT <u>ANYAQKFQGR</u> VTITADKSTSTAYMELSSLRSEDTAVYYC <u>ARAP</u>	100
<u>LR</u> FLEW <u>STQ</u> DH <u>YYYYYMDV</u> WGKGTTTVTVSS	130

Figure 2. 2F8 heavy chain amino acid sequence
CDRs in bold and underlined

<u>ATGGGATGGTCATGTATCATCCTTTTCTAGTAGCAACTGCAACTGGAGT</u>	50
<u>ACATTCAGAGGTCCAGCTGGTGCAGTCTGGGGCTGAGGTGAAGAAGCCTG</u>	100
<u>GGTCCTCGGTGAAGGTCTCCTGCAAGGCTTCTGGAGGCACCTTCAGCAGC</u>	150
<u>TATGCTATCAGCTGGGTGCGACAGGCCCTGGACAAGGGCTTGAGTGGAT</u>	200
<u>GGGAGGGATCATCCCTATCTTTGGTACAGCAAACCTACGCACAGAAGTTCC</u>	250
<u>AGGGCAGAGTCACGATTACCGCGGACAAATCCACGAGCACAGCCTACATG</u>	300
<u>GAGCTGAGCAGCCTGAGATCTGAGGACACGGCCGTGTATTACTGTGCGAG</u>	350
<u>AGCGCCATTACGATTTTTTGGAGTGGTCCACCCAAGACCACTACTACTACT</u>	400
<u>ACTACATGGACGTCTGGGGCAAAGGGACCACGGTCACCGTCTCAAGCGCC</u>	450
<u>TCCACCAAGGGGCCATCGGTCTTCCCCCTGGCACCCCTCCTCCAAGAGCAC</u>	500
<u>CTCTGGGGGCAAGCGGCCCTGGGCTGCCTGGTCAAGGACTACTTCCCCG</u>	550
<u>AACCGGTGACGGTGTCTGGAACCTCAGGCGCCCTGACCAGCGGCGTGAC</u>	600
<u>ACCTTCCCCGGCTGTCTTACAGTCTCAGGACTCTACTCCCTCAGCAGCGT</u>	650
<u>GGTGACCGTGCCCTCCAGCAGCTTGGGCACCCAGACCTACATCTGCAACG</u>	700
<u>TGAATCACAAGCCCAGCAACACCAAGGTGGACAAGAAAGTTGAGCCCCAA</u>	750
<u>TCTTGTGACAAAACCTCACACATGCCACCGTGCCCAGCACCTGAACTCCT</u>	800
<u>GGGGGGACCGTCAGTCTTCTCTTCCCCCAAAACCAAGGACACCCTCA</u>	850
<u>TGATCTCCCCGACCCCTGAGGTCACATGCGTGGTGGTGGACGTGAGCCAC</u>	900
<u>GAAGACCCTGAGGTCAAGTTCAACTGGTACGTGGACGGCGTGGAGGTGCA</u>	950
<u>TAATGCCAAGACAAAGCCGCGGGAGGAGCAGTACAACAGCACGTACCGGG</u>	1000
<u>TGGTCAGCGTCTCACCCTCCTGCACCAGGACTGGCTGAATGGCAAGGAG</u>	1050
<u>TACAAGTGCAAGGTCTCCAACAAAGCCCTCCCAGCCCCCATCGAGAAAAC</u>	1100
<u>CATCTCCAAGCCAAAGGGCAGCCCCGAGAACCACAGGTGTACACCCTGC</u>	1150
<u>CCCCATCCCCGGGAGGAGATGACCAAGAACCAGGTGAGCCTGACCTGCCTG</u>	1200
<u>GTCAAAGGCTTCTATCCCAGCGACATCGCCGTGGAGTGGGAGAGCAATGG</u>	1250
<u>GCAGCCGGGAGAACAACCTACAAGACCACGCCTCCCGTGCTGGACTCCGACG</u>	1300
<u>GCTCCTTCTTCTCTACAGCAAGCTCACCGTGGACAAGAGCAGGTGGCAG</u>	1350
<u>CAGGGGAACGTCTTCTCATGCTCCGTGATGCATGAGGCTCTGCACAACCA</u>	1400
<u>CTACACGCAGAAGAGCCTCTCCCTGTCTCCGGGTAAATGA</u>	1440

Figure 3. Complete 2F8 Heavy chain, class IgG1 DNA sequence. Secretory signal sequence (underlined), variable region (normal), IgG1 constant region (italics)

MGWSCIIILFLVATATGVHSEVQLVQSGAEVKKPGSSVKVSKASGGTFSS	50
<u>YAI</u> SWVRQAPGQGLEWMGGIIPIFGTANYA QK FO GRVTITADKSTSTAYM	100
ELSSLRSEDTAVYYCAR APLR FLEW ST QD HY Y Y Y MD VWGKGTTTVTVSSA	150
STKGPSVFPLAPSSKSTSGGTAALGCLVKDYFPEPVTVSWNSGALTSGVH	200
TFPAVLQSSGLYSLSSVTVPSSSLGTQTYICNVNHKPSNTKVDKKVEPK	250
SCDKTHTCPPCPAPELLGGPSVFLFPPKPKDTLMISRTPEVTCVVDVSH	300
EDPEVKFNWYVDGVEVHNAKTKPREEQYNSTYRVVSVLTVLHQDWLNGKE	350
YKCKVSNKALPAPIEKTI SKAKG QPREPQVYTLPPSREEMTKNQVSLTCL	400
VKGFPYPSDIAVEWESNGQPENNYKTPPVLDSDGSFFLYSKLTVDKSRWQ	450
QGNVFSCSVMEALHNHYTQKSLSLSPGK	479

Figure 4. Complete 2F8 Heavy chain, class IgG1 amino acid sequence. Secretory signal sequence (underlined), variable region (normal), CDRs (bold), IgG1 constant region (italics)

TCTTCTGAGCTGACTCAGGACCCCTGCTGTGTCTGTGGCCTTGGGACAGAC	50
AGTCAGGATCACATGCCAAGGAGACAGCCTCAGAAGCTATTATGCAAGCT	100
GGTACCAGCAGAAGCCAGGACAGGCCCTGTACTTGTCATCTATGGTAAA	150
AACAACCGGCCCTCAGGGATCCCAGACCGATTCTCTGGCTCCAGCTCAGG	200
AAACACAGCTTCCTTGACCATCACTGGGGCTCAGGCGGAAGATGAGGCTG	250
ACTATTACTGTAACCTCCCGGACAACAGTGATAACCGTCTGATATTGGC	300
GGCGGGACCAAGCTGACCGTCCTCAGT	327

Figure 5. 2F8 light chain variable region DNA sequence

SSELTQDPAVSVALGQTVRITC <u>QGDSLRSYYAS</u> WYQQKPGQAPVLVIY <u>GK</u>	50
<u>NNRPS</u> GIPDRFSGSSSGNTASLTITGAQAEDADYYC <u>NSRDNSDNRLIFG</u>	100
GGTKLTVLS	109

Figure 6. 2F8 light chain variable region amino acid sequence, CDRs (bold and underlined)

<u>ATGGGATGGTCATGTATCATCCTTTTCTAGTAGCAACTGCAACTGGAGT</u>	50
<u>ACATTCATCTTCTGAGCTGACTCAGGACCCTGCTGTGTCTGTGGCCTTGG</u>	100
GACAGACAGTCAGGATCACATGCCAAGGAGACAGCCTCAGAAGCTATTAT	150
GCAAGCTGGTACCAGCAGAAGCCAGGACAGGCCCTGTACTTGTCTATCTA	200
TGGTAAAAACAACCGGCCCTCAGGGATCCCAGACCGATTCTCTGGCTCCA	250
GCTCAGGAAACACAGCTTCCTTGACCATCACTGGGGCTCAGGCGGAAGAT	300
GAGGCTGACTATTACTGTAACCTCCCGGACAAACAGTGATAACCGTCTGAT	350
ATTTGGCGGCGGGACCAAGCTGACCGTCCTCAGTCAGCCCAAGGCTGCCC	400
<i>CCTCGGTCACTCTGTTCCCGCCCTCCTCTGAGGAGCTTCAAGCCAACAAG</i>	450
<i>GCCACACTGGTGTGTCTCATAAGTGACTTCTACCCGGGAGCCGTGACAGT</i>	500
<i>GGCCTGGAAGGCAGATAGCAGCCCCGTCAAGGCGGGAGTGGAGACCACCA</i>	550
<i>CACCTCCAAACAAGCAACAACAAGTACGCGGCCAGCAGCTATCTGAGC</i>	600
<i>CTGACGCTGAGCAGTGAAGTCCACAGAAGCTACAGCTGCCAGGTCAC</i>	650
<i>GCATGAAGGGAGCACCGTGGAGAAGACAGTGGCCCTGCAGAATGCTCTT</i>	700
GA	702

Figure 7. Complete 2F8 Light chain, lambda, DNA sequence. Secretory signal sequence (underlined), variable region (normal), lambda constant region (italics)

<u>MGWSCIIILFLVATATGVHSSSELTQDPAVSVALGQTVRITCQGDSLRSYY</u>	50
<u>ASWYQQKPGQAPV</u> LVIY GKNRPS GIPDRFSGSSSGNTASLTITGAQAED	100
EADYY CNSRDNSDNRL IFGGG TKLTVLSQPKA PSVTL FPPSSEELQANK	150
ATLVCLISDFYPGAVTV AWKADSSPVKAGVET TPSK QSN NKYAASSYLS	200
LTPEQ WKSHRSYSCQVTHEGSTVEKT VAPAEC S	233

Figure 8. Complete 2F8 Light chain, lambda, amino acid sequence. Secretory signal sequence (underlined), variable region (normal), CDRs (bold), lambda constant region (italics)

TCTTCTGAGCTGACTCAGGACCCTGCTGTGTCTGTGGCCTTGGGACAGAC	50
AGTCAGGATCACATGCCAAGGAGACAGCCTCAGAAGCTATTATGCAACCT	100
GGTACCAGCAGAAGCCAGGACAGGCCCTATTCTTGTCTATCTATGGTGAA	150
AATAAGCGGCCCTCAGGGATCCCAGACCGATTCTCTGGCTCCAGCTCAGG	200
AAACACAGCTTCCTTGACCATCACTGGGGCTCAGGCAGAAGATGAGGCTG	250
ACTACTATTGTAAATCTCGGGATGGCAGTGGTCAACATCTGGTGTTCGGC	300
GGAGGGACCAAGCTGACCGTCCTAGGT	327

Figure 9. A12 light chain variable region DNA sequence

SSELTQDPAVSVALGQTVRITC QGDSLRSYY ATWYQQKPGQAPILVIYGE	50
NKRPSGI PDRFSGSSSGNTASLTITGAQAEDADYY CKSRDGS QH LVFG	100
GGTKLTVLG	109

Figure 10. A12 light chain variable region amino acid sequence, CDRs (bold and underlined)

<u>ATGGGATGGTCATGTATCATCCTTTTTCTAGTAGCAACTGCAACTGGAGT</u>	50
<u>ACATTCACTTTCTGAGCTGACTCAGGACCCCTGCTGTGTCTGTGGCCTTGG</u>	100
GACAGACAGTCAGGATCACATGCCAAGGAGACAGCCTCAGAAGCTATTAT	150
GCAACCTGGTACCAGCAGAAGCCAGGACAGGCCCTATTCTTGTCATCTA	200
TGGTGAAAATAAGCGGCCCTCAGGGATCCCAGACCGATTCTCTGGCTCCA	250
GCTCAGGAAACACAGCTTCCTTGACCATCACTGGGGCTCAGGCAGAAGAT	300
GAGGCTGACTACTATTGTAAATCTCGGGATGGCAGTGGTCAACATCTGGT	350
GTTTCGGCGGAGGGACCAAGCTGACCGTCCTAGGTCAGCCCAAGGCTGCCC	400
<i>CCTCGGTCACTCTGTTCCCGCCCTCCTCTGAGGAGCTTCAAGCCAACAAG</i>	450
<i>GCCACACTGGTGTGTCTCATAAGTGACTTCTACCCGGGAGCCGTGACAGT</i>	500
<i>GGCCTGGAAGGCAGATAGCAGCCCCGTCAAGGCGGGAGTGGAGACCACCA</i>	550
<i>CACCCCTCAAACAAGCAACAACAAGTACGCGGCCAGCAGCTATCTGAGC</i>	600
<i>CTGACGCCTGAGCAGTGAAGTCCACAGAAGCTACAGCTGCCAGGTCAC</i>	650
<i>GCATGAAGGGAGCACCGTGGAGAAGACAGTGGCCCCCTGCAGAATGCTCTT</i>	700
GA	702

Figure 11. Complete A12 Light chain, lambda, DNA sequence. Secretory signal sequence (underlined), variable region (bold), lambda constant region (italics)

<u>MGWSCIIILFLVATATGVHSSSELTQDPAVSVALGQTVRITCQGDSLRSYY</u>	50
<u>ATWYQQKPGQAPILVIYGENKRPSGI</u> PDRFSGSSSGNTASLTITGAQAED	100
EADYY CKSRDGS QH LVFGGGTKLTVLGQPKAAPSVTLFPPSSEELQANK	150
ATLVCLISDFYPGAVTVAWKADSSPVKAGVETTTPSKQSNKYAASSYLS	200
LTPEQWKSHRSYSCQVTHEGSTVEKTVAPAECS	233

Figure 12. Complete A12 Light chain, lambda, amino acid sequence. Secretory signal sequence (underlined), variable region (normal), CDRs (bold), lambda constant region (italics)

Heavy chain			
CDR1	CDR2	CDR3	
SYAIS	GIIPIFGTANYAQKFQG	APLRFLEWSTQDHYYYYYMDV	2F8/A12
Light chain			
CDR1	CDR2	CDR3	
QGDSLRSYYAS	<u>G</u> <u>K</u> <u>N</u> <u>N</u> <u>R</u> <u>P</u> <u>S</u>	<u>N</u> <u>S</u> <u>R</u> <u>D</u> <u>N</u> <u>S</u> <u>D</u> <u>N</u> <u>R</u> <u>L</u> <u>I</u>	2F8
QGDSLRSYYAT	<u>G</u> <u>E</u> <u>N</u> <u>K</u> <u>R</u> <u>P</u> <u>S</u>	<u>K</u> <u>S</u> <u>R</u> <u>D</u> <u>G</u> <u>S</u> <u>G</u> <u>Q</u> <u>H</u> <u>L</u> <u>V</u>	A12

Figure 13. 2F8 and A12 variable region complementarity determining regions (CDRs), differences in light CDRs sequences are underlined

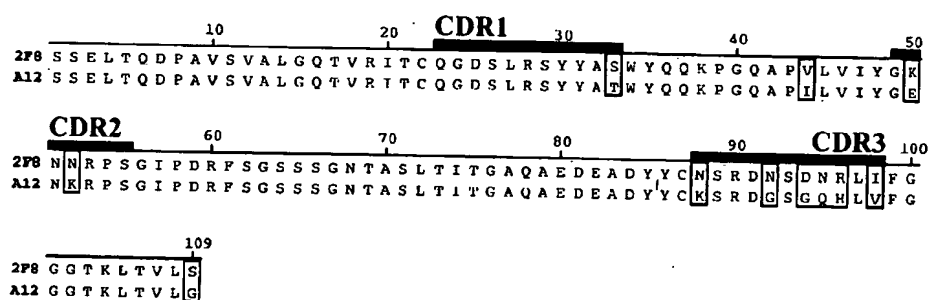


Figure 14. Homology alignment of light chain variable region amino acid sequences. Differing amino acid residues are boxed and CDRs are highlighted.

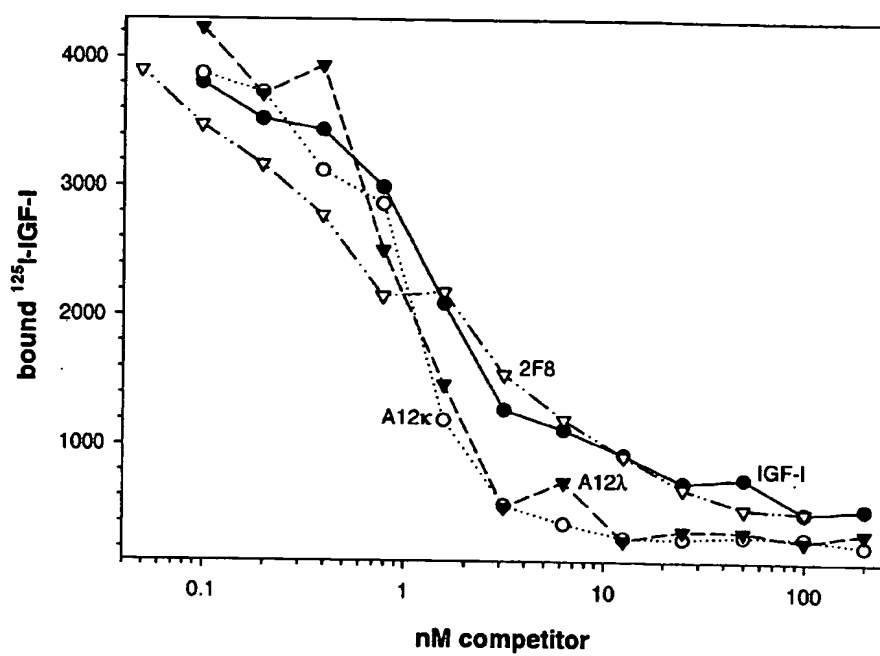


Figure 15. *In vitro* IGF-I ligand blocking assay to immobilized human soluble IGF-IR.

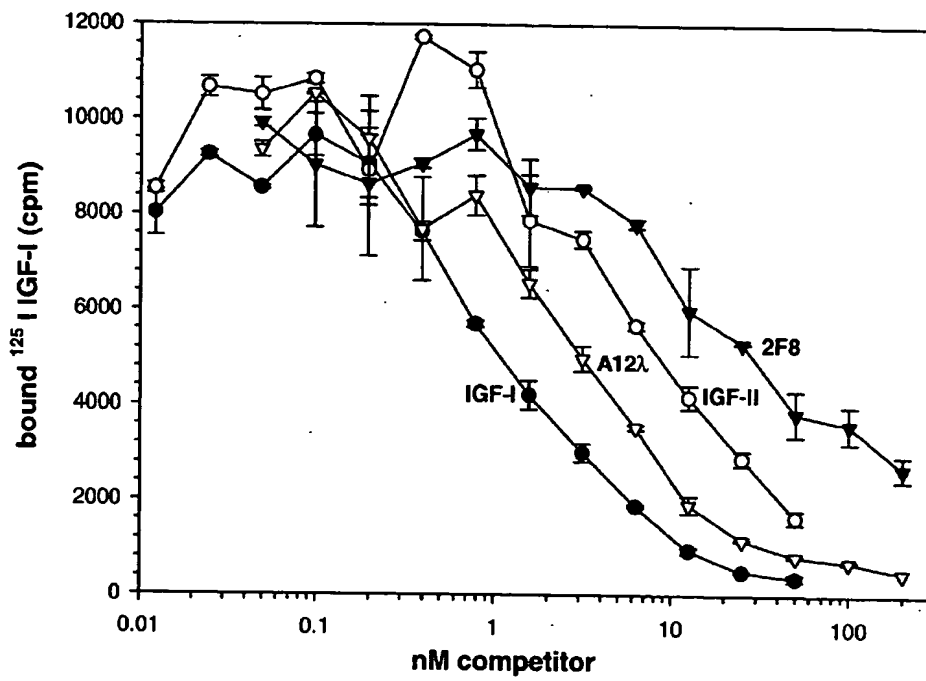


Figure 16. Cell-based IGF-I ligand blocking assay on MCF7 cells.

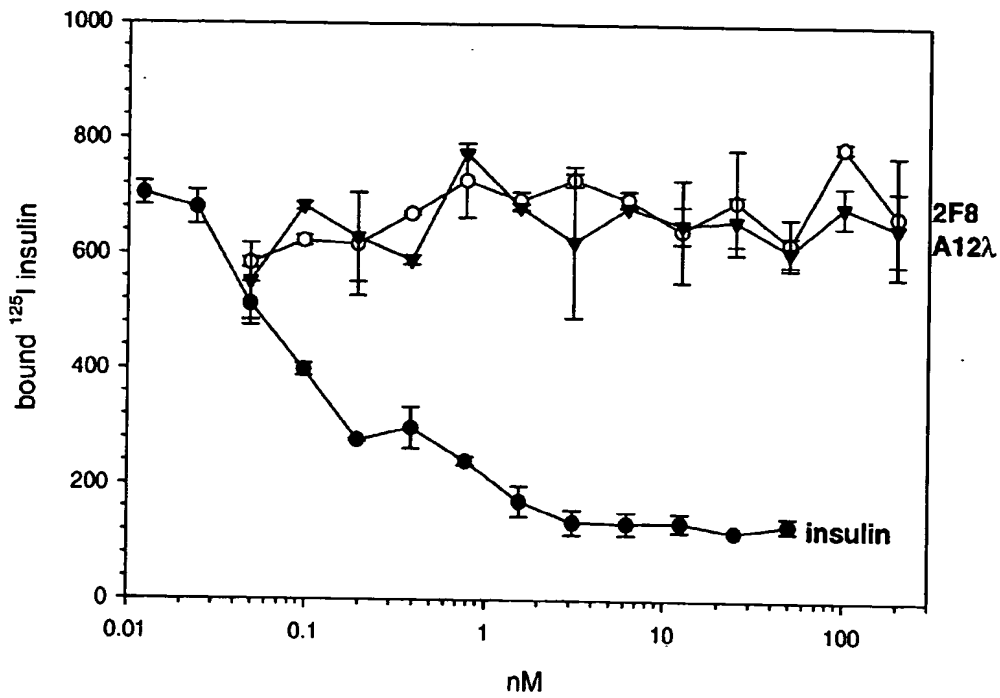


Figure 17. Cell-based insulin ligand blocking assay on ZR75-I cells.

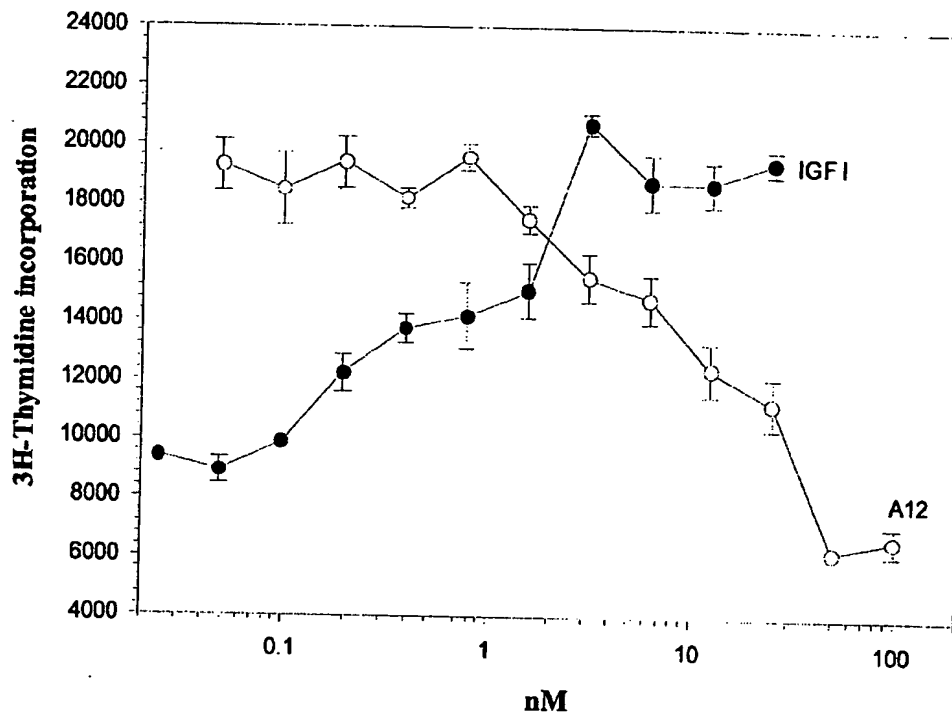


Figure 18. *In vitro* mitogenesis assay on MCF7 breast cancer cells.

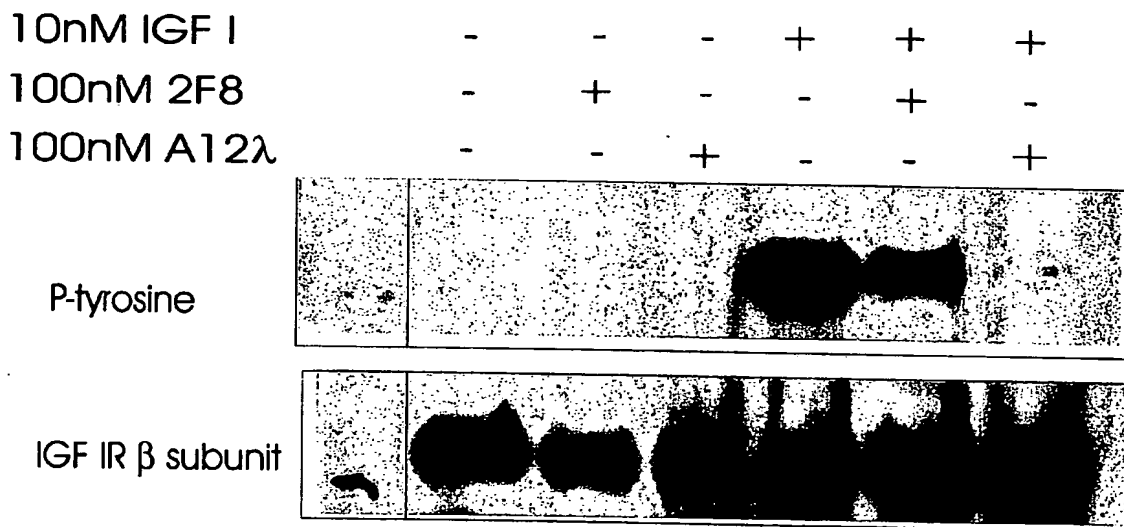
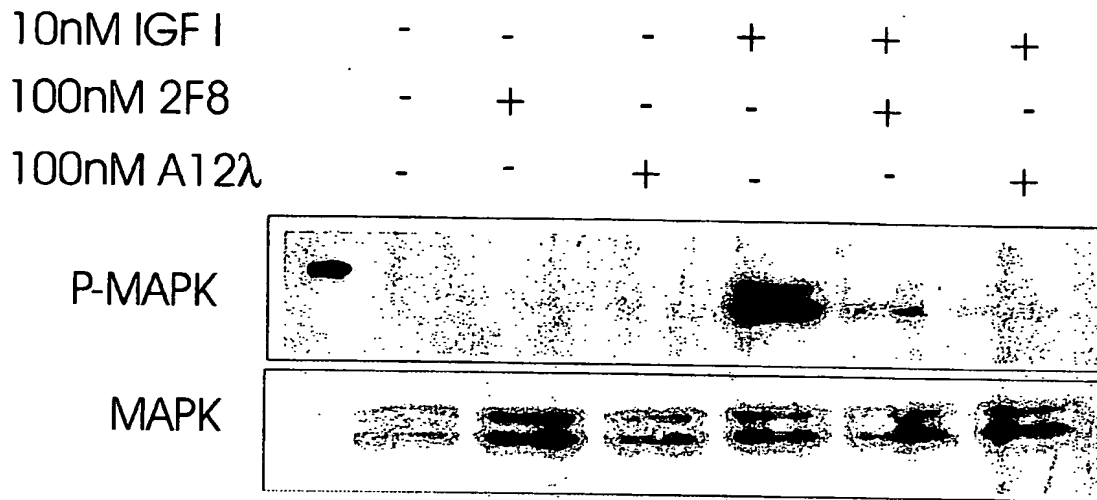
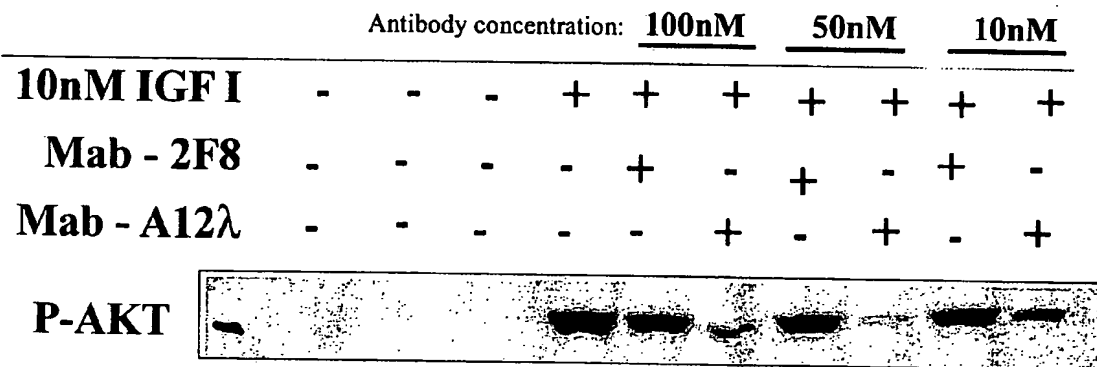


Figure 19. Inhibition of IGF-I-mediated receptor auto-phosphorylation by antibody A12 and 2F8 in human MCF7 breast cancer cell line.



A.



B.

Figure 20. Inhibition of IGF-I-mediated down-stream effector molecule phosphorylation by antibody A12 and 2F8.

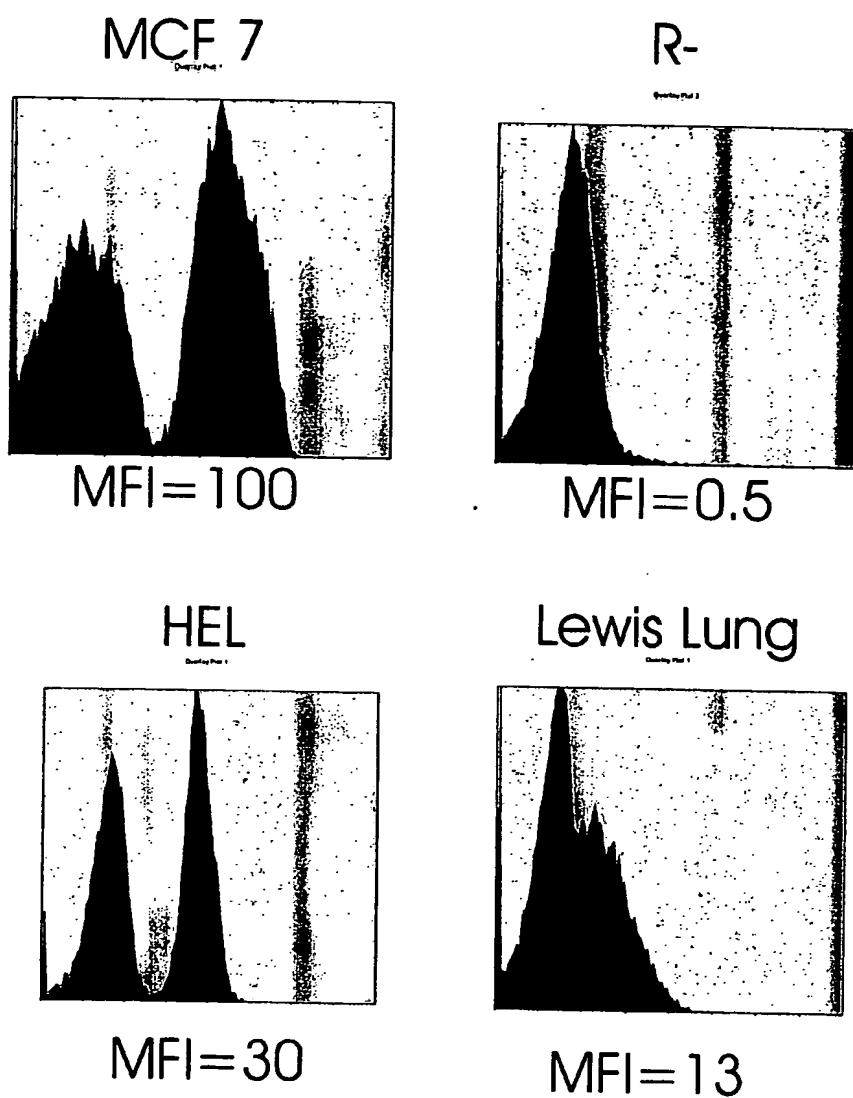


Figure 21. FACS comparison of antibody A12 binding to IGF-IR positive or negative cell lines.

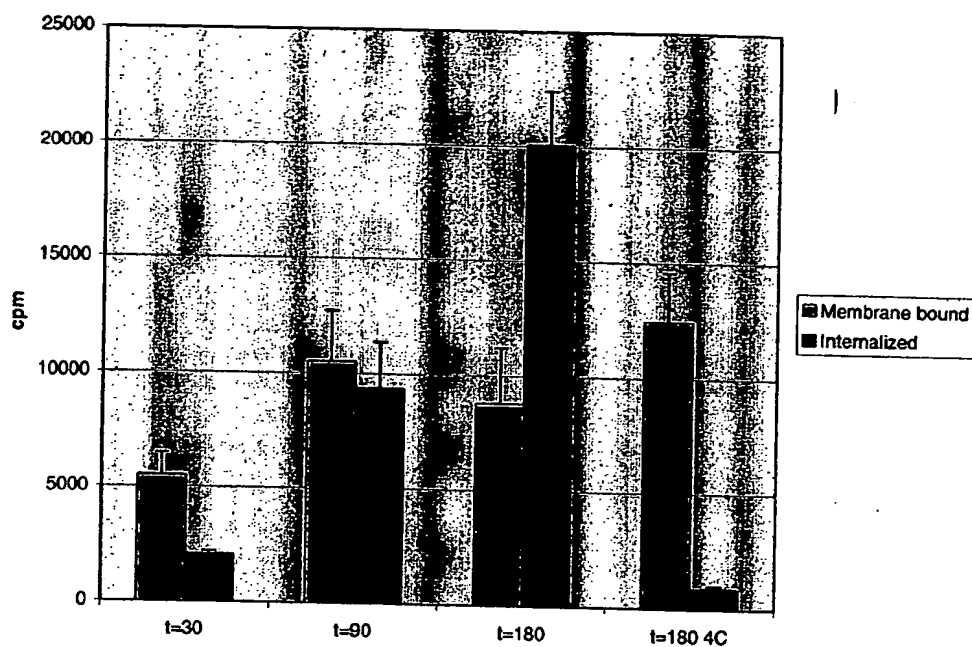


Figure 22. Antibody A12 internalization following binding to IGF-I receptor on MCF7 cells.

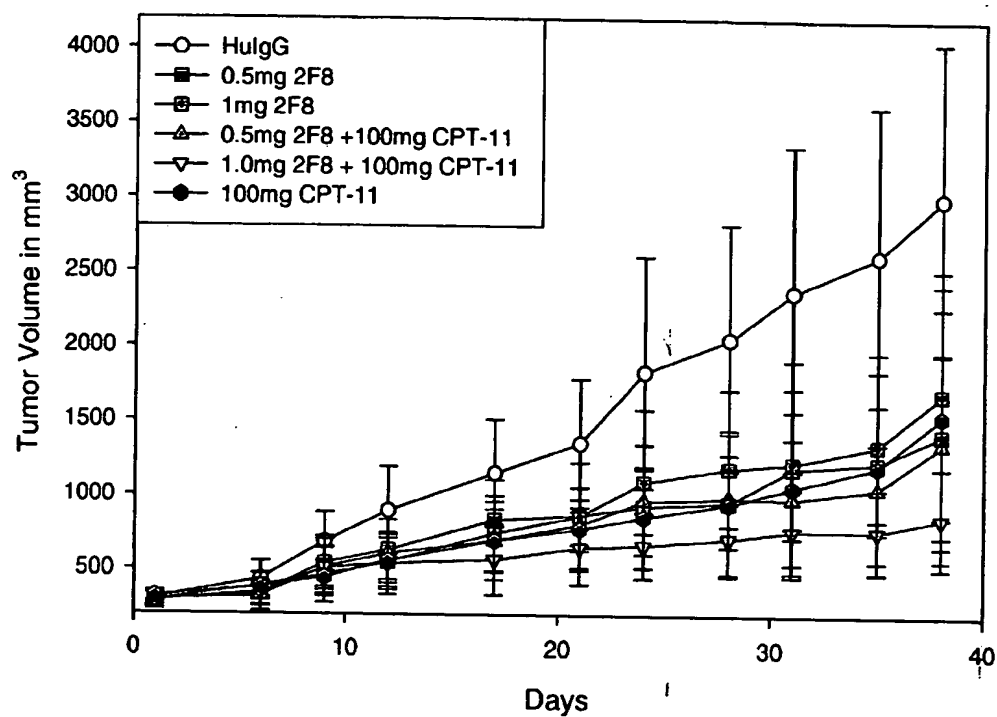


Figure 23. Inhibition of HT-29 human colon carcinoma growth in nude mice by antibody 2F8 alone or in combination with CPT-11.

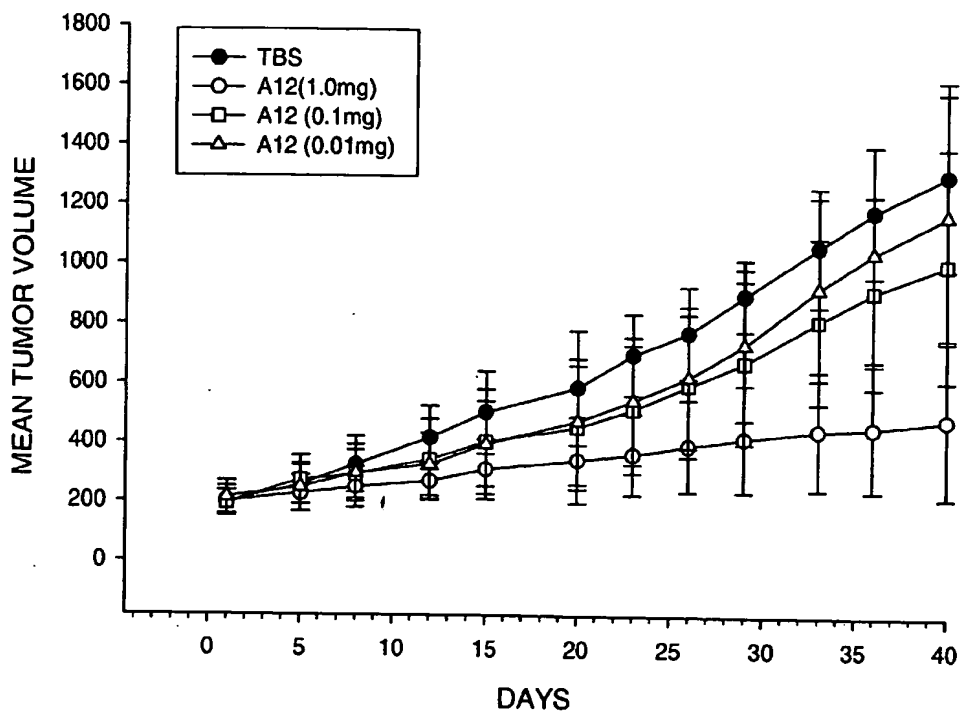


Figure 24. Effect of A12 therapy on HT-29 human colorectal tumor growth in nude mice.

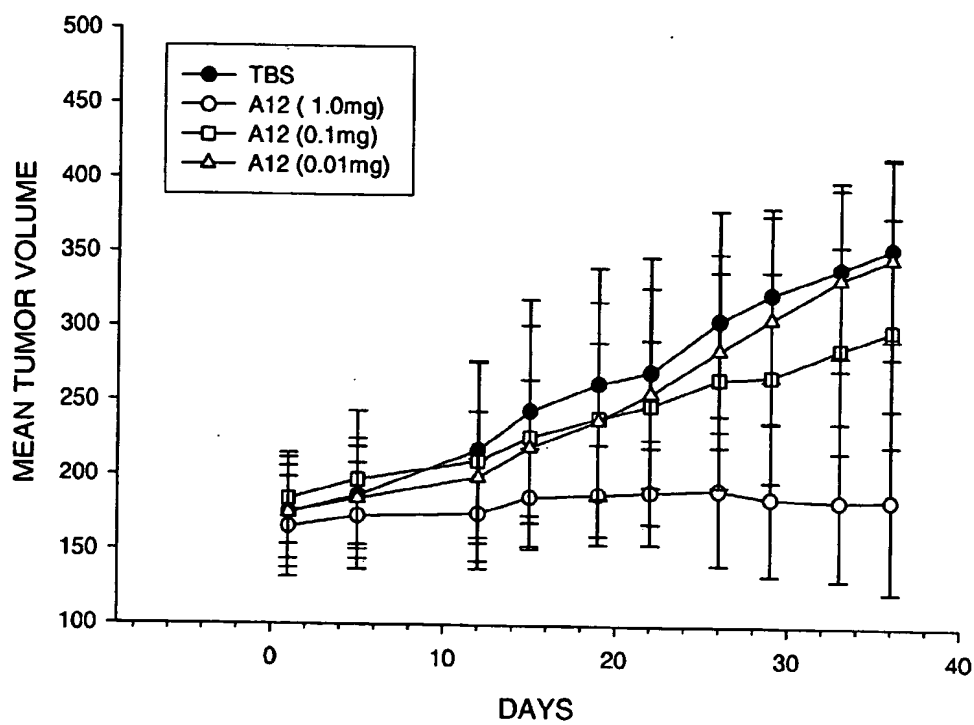


Figure 25. Effect of A12 therapy on MCF7 human breast cancer growth in nude mice.

Document made available under the Patent Cooperation Treaty (PCT)

International application number: PCT/US04/013852

International filing date: 03 May 2004 (03.05.2004)

Document type: Certified copy of priority document

Document details: Country/Office: US
Number: 60/467,177
Filing date: 01 May 2003 (01.05.2003)

Date of receipt at the International Bureau: 08 October 2004 (08.10.2004)

Remark: Priority document submitted or transmitted to the International Bureau in compliance with Rule 17.1(a) or (b)



World Intellectual Property Organization (WIPO) - Geneva, Switzerland
Organisation Mondiale de la Propriété Intellectuelle (OMPI) - Genève, Suisse

**This Page is Inserted by IFW Indexing and Scanning
Operations and is not part of the Official Record**

BEST AVAILABLE IMAGES

Defective images within this document are accurate representations of the original documents submitted by the applicant.

Defects in the images include but are not limited to the items checked:

- ☒ BLACK BORDERS
 - ☐ IMAGE CUT OFF AT TOP, BOTTOM OR SIDES
 - ☐ FADED TEXT OR DRAWING
 - ☐ BLURRED OR ILLEGIBLE TEXT OR DRAWING
 - ☐ SKEWED/SLANTED IMAGES
 - ☐ COLOR OR BLACK AND WHITE PHOTOGRAPHS
 - ☐ GRAY SCALE DOCUMENTS
 - ☐ LINES OR MARKS ON ORIGINAL DOCUMENT
 - ☐ REFERENCE(S) OR EXHIBIT(S) SUBMITTED ARE POOR QUALITY
-
- ☐ OTHER: _____

IMAGES ARE BEST AVAILABLE COPY.

As rescanning these documents will not correct the image problems checked, please do not report these problems to the IFW Image Problem Mailbox.